

Pedro R. S. Antunes and Edouard Oudet

# Numerical results for extremal problem for eigenvalues of the Laplacian

We consider in this chapter shape optimization problems for Dirichlet and Neumann eigenvalues,

$$\lambda_i^* := \min \left\{ \lambda_i(\Omega), \Omega \subset \mathbb{R}^d, |\Omega| = 1 \right\}, i = 1, 2, \dots \quad (1)$$

and

$$\mu_i^* := \max \left\{ \mu_i(\Omega), \Omega \subset \mathbb{R}^d, |\Omega| = 1 \right\}, i = 2, 3, \dots \quad (2)$$

Some of these shape optimizations have already been solved. The first Dirichlet eigenvalue is minimized by the ball, as proven by Faber and Krahn [262, 428]. The second Dirichlet eigenvalue is minimized by two balls of the same volume [429]. In two dimensional case, it has long been conjectured that the ball minimizes  $\lambda_3(\Omega)$ , but there has not been much progress in this direction. For higher eigenvalues, not much is known and even the existence of minimizers among quasi-open sets has only been proven quite recently (see Chapter 2) and [146, 496]. It is worth mentioning the work by Berger [88] who proved that for  $i > 4$ , the  $i$ -th Dirichlet eigenvalue is not minimized by any union of balls.

For the Neumann problem, we have  $\mu_1(\Omega) = 0$ . The second eigenvalue,  $\mu_2(\Omega)$ , is maximized by the ball. The result had been conjectured by Kornhauser and Stakgold in [424] and was proved by Szegő in [592] for Lipschitz simply connected planar domains and generalized by Weinberger in [614] to arbitrary domains, and any dimension. More recently, Girouard, Nadirashvili and Polterovich proved that the maximum of  $\mu_3(\Omega)$  among simply connected bounded planar domains is attained by two disjoint balls of equal area [299].

Recently, many works have addressed numerical approaches that propose candidates for the optimizers for these and related spectral problems, and to suggest conjectures about their qualitative properties [28, 103, 516, 517, 518, 519].

In the next two sections we describe briefly two of these approaches which have been successful for spectral problems. We first introduce some global optimization tools to provide a good initial guess of the optimal profile. This step does not require any topological information on the set but is restricted to a small class of shapes. Moreover, since this approach relies only on the parametrization of the space of shapes, any global algorithm can be used as a black box solver to find a starting candidate for the

---

**Pedro R. S. Antunes:** Grupo de Física Matemática da Universidade de Lisboa, Portugal, E-mail: prantunes@fc.ul.pt

**Edouard Oudet:** Laboratoire Jean Kuntzmann (LJK), Université Joseph Fourier et CNRS, Tour IRMA, BP 53, 51 rue des Mathématiques, 38041 Grenoble Cedex 9 - France, E-mail: edouard.oudet@imag.fr



© 2016 Pedro R. S. Antunes and Edouard Oudet

This work is licensed under the Creative Commons Attribution-NonCommercial-NoDerivs 3.0 License.

local procedure. We then describe the method of fundamental solutions which is able in a second stage to both identify and evaluate precisely shapes which are locally optimal.

## 1 Some tools for global numerical optimization in spectral theory

Global optimality is perhaps one of the most challenging aspects in numerical shape optimization. Many approaches have been developed to tackle this difficulty: stochastic algorithms, multi scale methods, relaxation, homogenization, etc. In this section we first recall briefly an historical method developed to apply a genetic algorithm in the framework of shape optimization. It has the benefit of dramatically reducing the number of degrees of freedom, which makes the global optimization more efficient, it has the drawback of parametrizing non smooth profiles.

In the following we introduce a very naive approach based on implicit representation which makes it possible both to reduce the number of unknowns and to generate smooth shapes. In a second step we describe a new simple idea to restrict the search space in spectral optimization to one where homogeneous functionals are frequently involved.

### 1.1 An historical approach: Genetic algorithm and Voronoi cells

Consider a given grid covering a search domain in which we look for an optimal shape  $\Omega$ . A purely discrete numerical approach consists of associating to every node of the grid a boolean value which expresses the fact that the node is or is not in the set  $\Omega$ .

In the 90's, Allaire et al. [14] introduced a discretization framework in shape optimization based on Voronoi cells associated to a set of points independent of the grid. In this setting a grid point of the search space is considered to be a part of  $\Omega$  if the seed of its Voronoi cell has a True boolean value. The interesting part of this method is that the complexity of the approach is not anymore related to the grid size but only on the number of seed points. This crucial distinction makes it possible to compute state solutions of partial differential equations with a reasonable precision whereas the number of unknowns is not too large. A drawback of the method is the non smoothness of Voronoi cells. Due to its polygonal faces, an large number of Voronoi seeds may be required to approximate smooth shapes. In the specific context of eigenvalues where some smoothness is expected, this kind of discretization is not optimal.

## 1.2 Smooth profiles with few parameters

In this section related to global spectral optimization we consider the minimization of functional of the type

$$G(\Omega) = F(|\Omega|, |\partial\Omega|, \{\lambda_i(\Omega)\}_{1 \leq i \leq k}, \{\mu_i(\Omega)\}_{1 \leq i \leq l}) \quad (3)$$

where  $F$  is some smooth fixed finite dimensional function. We address the optimization problem

$$\min_{\Omega} G(\Omega). \quad (4)$$

Depending on the context we may consider additional geometrical constraints imposed on the set  $\Omega$  like a fixed measure or boundary measure, connectivity, convexity, etc.

Identifying the global optimal solution of a non convex and sometimes non smooth cost function is in almost all cases an untenable task. In order to decrease the complexity of this problem we introduce a reduction of the number  $mp$  of parameters which still allows a precise computation of the cost function. Since we use black box stochastic algorithm we need to reduce the number of parameters to  $mp \leq 100$  for instance. More precisely we develop this dimension reduction by introducing the two following steps.

In the spirit of level set methods, we first parameterize the set of shape as the level sets of truncated Fourier series. Contrary to standard boundary parametrization where the number of degrees of freedom is related to the number of boundary points in the mesh, our parametrization has the complexity of the number of terms in the Fourier series. Moreover, the very basic and crucial observation is the fact that this complexity is not related to the precision of the eigenvalue approximation.

Our second improvement is related to the reduction of the size of the search space. We reduce the complexity of the optimization process by substituting the cost evaluation of a given shape by the optimal value associated to the best homothetic connected components. Essentially it relies on the two following classical properties:

**Proposition 1.1** (Homogeneity). *Let  $\alpha > 0$  be a real. Then for all integers  $j$ ,*

$$\lambda_j(\alpha\Omega) = \alpha^{-2}\lambda_j(\Omega), \quad \mu_j(\alpha\Omega) = \alpha^{-2}\mu_j(\Omega), \quad |\alpha\Omega| = \alpha^d|\Omega| \quad \text{and} \quad |\partial(\alpha\Omega)| = \alpha^{d-1}|\partial\Omega|. \quad (5)$$

Notice that homogeneity can be used to a transform constrained problem like

$$\min\{\lambda_i(\Omega), |\Omega| = 1\}, \quad i = 1, 2, \dots \quad (6)$$

into an unconstrained one

$$\min\{\lambda_i(\Omega)|\Omega|\}, \quad i = 1, 2, \dots \quad (7)$$

The second property makes it possible to compute more efficiently optimal profiles with multiply connected components:

**Proposition 1.2** (Multiply connected components). *Let  $\Omega_1, \dots, \Omega_m$  be the connected components of  $\Omega$ . For  $i = 1, \dots, m$ , let  $\Lambda_i$  be the set of the eigenvalues of  $-\Delta$  on  $\Omega_i$  for Dirichlet or Neumann condition. Then the set of the eigenvalues of  $\Delta$  is  $\Lambda = \bigcup_{i=1}^m \Lambda_i$ .*

We now describe our discretization of the search space for  $d = 2$ . The generalization to higher dimensions is straightforward. Let us consider coefficients  $a_{i,j}$  such that  $\sharp\{a_{i,j}\} = n$  (the number of coefficients). Then, define the Fourier series

$$\Phi_{\{a_{i,j}\}}(x) = \sum_{i,j} a_{i,j} \sin(\pi i x_1) \sin(\pi j x_2) + 1, \quad \text{where } x = (x_1, x_2) \in [0, 1]^2. \quad (8)$$

Notice that we add the constant value 1 to previous sum so that the function is non-zero on  $\partial\Omega$ . That is the level set domain does not intersect the boundary. We now define  $\mathcal{F} : \mathbb{R}^n \rightarrow \mathcal{P}(\mathbb{R}^2)$  by

$$\mathcal{F}(\{a_{i,j}\}) = \{x \in [0, 1]^2, \Phi_{\{a_{i,j}\}}(x) \leq 0\}. \quad (9)$$

Finally we build the sets

$$\Omega_{\{a_{i,j}\}} = \mathcal{F}(\{a_{i,j}\}). \quad (10)$$

Notice that the topology or more specifically the number of connected components of  $\Omega_{\{a_{i,j}\}}$  is not imposed by the algorithm.

In practice,  $B = [0, 1]^2$  is meshed by a Cartesian grid.  $\Phi_{\{a_{i,j}\}}$  is evaluated at every point of the mesh and a linear interpolation is carried out to approximate  $\mathcal{F}(\{a_{i,j}\})$ . Through this discretization we associate a polygon  $\Omega_{\{a_{i,j}\}}^{pol}$  to every  $\Omega_{\{a_{i,j}\}}$ . We then define the cost function associated to the parameters  $a_{i,j}$  by

$$F(\{a_{i,j}\}) := G(\Omega_{\{a_{i,j}\}}^{pol}) \simeq G(\Omega_{\{a_{i,j}\}}) = G(\mathcal{F}(\{a_{i,j}\})).$$

Where the  $\simeq$  symbol expresses the fact we do not optimize the true eigenvalues of the polygons in this process but rather the finite element approximation of these eigenvalues. Finally, it is standard to approximate the cost function  $G(\Omega_{\{a_{i,j}\}}^{pol})$  by classical Finite Element Methods. Notice that every evaluation requires us to construct a new mesh adapted to the polygon  $\Omega_{\{a_{i,j}\}}^{pol}$  since linear interpolation generates meshes of very bad quality. In all our experiments we fixed approximately the number of simplices per evaluation to obtain comparable results.

### 1.3 A fundamental complexity reduction: optimal connected components

We detailed in previous section a way to parametrize multi-connected shapes with few parameters. As it has been explained, every cost evaluation requires to mesh the new domain and to solve the associated discrete spectral optimization problem. This step can be very time-consuming especially in the case of 3 dimension computations.

To tackle this difficulty, we would like to use the homogeneity of eigenmodes to investigate homothetical components in one single cost evaluation. Actually, due to the homogeneity of eigenmodes the computation of these modes associated to one geometrical configuration can be used to deduce the cost function of any domain made of homothetic components.

From properties 1.1 and 1.2 we obtain that if  $\Omega = \alpha_1 \Omega_1 \cup \alpha_2 \Omega_2$  (disjoint union) then

$$\begin{aligned} G(\alpha_1 \Omega_1 \cup \alpha_2 \Omega_2) &= F(|\Omega|, |\partial\Omega|, \{\lambda_i(\Omega)\}_{1 \leq i \leq k}, \{\mu_i(\Omega)\}_{1 \leq i \leq l}) \\ &= F(\alpha_1^d |\Omega_1| + \alpha_2^d |\Omega_2|, \alpha_1^{d-1} |\partial\Omega_1| + \alpha_2^{d-1} |\partial\Omega_2|, \dots \\ &\quad \{\lambda_i(\alpha_1 \Omega_1 \cup \alpha_2 \Omega_2)\}_{1 \leq i \leq k}, \{\mu_i(\alpha_1 \Omega_1 \cup \alpha_2 \Omega_2)\}_{1 \leq i \leq l}) \end{aligned}$$

The crucial fact observation is that the computation of  $\lambda_j(\alpha_1 \Omega_1 \cup \alpha_2 \Omega_2)$  and  $\mu_j(\alpha_1 \Omega_1 \cup \alpha_2 \Omega_2)$  is equivalent to the sorting operation of the union of the two sets

$$\{\alpha_1^{-2} \lambda_i(\Omega_1); 1 \leq j \leq m < k\} \cup \{\alpha_2^{-2} \lambda_i(\Omega_2); 1 \leq j \leq k - m\}$$

and

$$\{\alpha_1^{-2} \mu_j(\Omega_1); 1 \leq j \leq m' < l\} \cup \{\alpha_2^{-2} \mu_j(\Omega_2); 1 \leq j \leq l - m'\}.$$

Let  $\Omega$  be a fixed set with  $m$  connected components. Let us associate to  $\Omega$  a new cost which is the best value obtained with respect to its homothetical connected components. More precisely we define:

$$G(\Omega_{\{a_{i,j}\}}^{pol}) = \min_{(\alpha_1, \dots, \alpha_m) \geq 0} G(\alpha_1 \Omega_1^{pol} \cup \dots \cup \alpha_m \Omega_m^{pol}) \quad (11)$$

where

$$\Omega_{\{a_{i,j}\}}^{pol} = \bigcup_{i=1}^m \Omega_i^{pol}. \quad (12)$$

Notice that due to the translation invariance of the problem we can always assume that every connected components are disjoint. As a consequence, we can associate to a fixed geometrical configuration with  $m$  connected components a new cost defined by (11). This small scale global problem (11) can be solved very efficiently by using global algorithm like Lipschitz optimization (see for instance [406]). Moreover, since the number of unknowns is small (the number of expected connected components) and the cost evaluation is pretty fast, this global optimization problem can be solved very quickly with respect to a finite element evaluation.

## 2 Numerical approach using the method of fundamental solutions

The eigenvalue problem for the Laplace operator is equivalent to obtaining the resonant frequencies  $0 \leq \kappa_1 \leq \kappa_2 \leq \dots \leq \kappa_p \leq \dots$  that lead to non trivial solutions of the

Helmholtz equation  $u_p \not\equiv 0$  :

$$\begin{cases} \Delta u_p + \kappa_p^2 u_p = 0 & \text{in } \Omega, \\ u_p = 0 \text{ or } \partial_n u = 0 & \text{on } \Gamma. \end{cases} \quad (13)$$

Among other numerical approaches, these eigenvalue problems can be solved by the Method of Fundamental Solutions (MFS) [20, 408]. The MFS is a Trefftz type method, where the particular solutions are point sources centered outside the domain. More precisely, denoting by  $\|\cdot\|$  the Euclidean norm in  $\mathbb{R}^d$ , we take a fundamental solution of the Helmholtz equation

$$\Phi_\kappa(x) = \frac{i}{4} H_0^{(1)}(\kappa \|x\|) \quad (14)$$

for the two-dimensional case, where  $H_0^{(1)}$  is the first Hankel function and

$$\Phi_\kappa(x) = \frac{e^{i\kappa\|x\|}}{4\pi \|x\|} \quad (15)$$

in the three-dimensional case. We have  $(\Delta + \kappa^2)\Phi_\kappa = -\delta$ , where  $\delta$  is the Dirac delta distribution. For a given frequency  $\kappa$ , we consider a basis built with point sources

$$\phi_j = \Phi_\kappa(\cdot - y_j) \quad (16)$$

where  $y_j \in \bar{\Omega}$ . By  $\hat{\Gamma} = \partial\hat{\Omega}$ , we will denote an admissible source set, for instance, the boundary of a bounded open set  $\hat{\Omega} \supset \bar{\Omega}$ , with  $\hat{\Gamma}$  surrounding  $\partial\Omega$ .

The MFS approximation is a linear combination

$$\sum_{j=1}^m \alpha_j \Phi_\kappa(\cdot - y_j), \quad (17)$$

where the source points  $y_j$  are placed on an admissible source set. The approximation of an eigenfunction by a MFS linear combination can be justified by density results (e.g. [20]),

**Theorem 2.1.** *Consider  $\hat{\Gamma} = \partial\hat{\Omega}$ , an admissible source set. Then,*

$$S(\hat{\Gamma}) = \text{span}\{\Phi_\kappa(\cdot - y)|_\Omega : y \in \hat{\Gamma}\}$$

*is dense in  $\mathcal{H}_\kappa(\Omega) = \{v \in H^1(\Omega) : (\Delta + \kappa^2)v = 0\}$ , with the  $H^1(\Omega)$  topology.*

Next we give a brief description of the application of the MFS for determining the eigensolutions for a given shape  $\Omega$ . For details, see [19] and [25] respectively for the two and three-dimensional cases. The eigensolutions are obtained in two steps. First, we calculate an approximate eigenfrequency  $\tilde{\kappa}$  and then, for that frequency, we obtain the approximation for the eigenfunction.

We define  $m$  collocation points  $x_i$  almost uniformly distributed on the boundary  $\partial\Omega$  and for each of those points we define a corresponding source point,

$$y_i = x_i + \alpha n_i,$$

where  $\alpha$  is a positive parameter and  $n_i$  is the unitary outward normal vector at the point  $x_i$ . Imposing the Dirichlet boundary conditions at the boundary points we obtain the system

$$\sum_{j=1}^m \alpha_j \Phi_\kappa(x_i - y_j) = 0. \quad (18)$$

A straightforward procedure for calculating the eigenfrequencies is to find the values  $\kappa$  for which the  $m \times m$  matrix

$$A(\kappa) = [\Phi_\kappa(x_i - y_j)]_{m \times m} \quad (19)$$

is singular. The Neumann case is similar.

To obtain an eigenfunction associated with a certain resonant frequency  $\kappa$  we use a collocation method on  $n + 1$  points, with  $x_1, \dots, x_n$  on  $\partial\Omega$  and a point  $x_{n+1} \in \Omega$ . The eigenfunction is approximated by an MFS approximation,

$$\tilde{u}(x) = \sum_{j=1}^{n+1} \alpha_j \Phi_\kappa(x - y_j) \quad (20)$$

and to exclude the trivial solution  $\tilde{u}(x) \equiv 0$ , the coefficients  $\alpha_j$  are determined by solving the system

$$\tilde{u}(x_i) = \delta_{i,n+1}, \quad i = 1, \dots, n + 1$$

where  $\delta_{i,j}$  is the Kronecker delta. An advantage of the Method of Fundamental Solutions approach with respect to Finite Element Method approach is the fact that we can calculate rigorous bounds for the errors associated to approximate eigenvalues. In the Dirichlet case, the error can be estimated by using an *a posteriori bound* due to Fox, Henrici and Moler (cf. [272]). This result provides upper bounds for the errors of the approximations obtained in several methods of particular solutions and was also used in rigorous proofs (eg. [19, 93, 461]).

Next, we define the class of admissible domains for the shape optimization. Note that if for some  $i = 1, 2, \dots$ , the optimizer of the problems (1) or (2) is disconnected, by Wolf-Keller Theorem (cf. [621]), each of the connected components are optimizers of a lower eigenvalue. Thus, we will focus on the numerical solution of the shape optimization problem among connected domains and then compare this optimal value against the optimal value obtained for disconnected sets by using Wolf-Keller theorem.

We consider the functions

$$\gamma_1(t) = a_0^{(1)} + \sum_{j=1}^P a_j^{(1)} \cos(jt) + \sum_{j=1}^P b_j^{(1)} \sin(jt)$$

and

$$\gamma_2(t) = a_0^{(2)} + \sum_{j=1}^P a_j^{(2)} \cos(jt) + \sum_{j=1}^P b_j^{(2)} \sin(jt),$$

for some  $P \in \mathbb{N}$  and the vector  $\mathcal{C} \in \mathbb{R}^{4P+2}$  with all the coefficients of these expansions,

$$\mathcal{C} = \left( a_0^{(1)}, a_1^{(1)}, \dots, a_P^{(1)}, b_1^{(1)}, \dots, b_P^{(1)}, a_0^{(2)}, a_1^{(2)}, \dots, a_P^{(2)}, b_1^{(2)}, \dots, b_P^{(2)} \right).$$

The class of planar admissible domains is the set

$$\mathcal{V} = \left\{ V \subset \mathbb{R}^2 : \partial V = (\gamma_1(t), \gamma_2(t)) : t \in [0, 2\pi] \text{ is a Jordan curve} \right\}.$$

For the three dimensional case, we assume that  $\Omega$  is star-shaped and its boundary can be parametrized by

$$\partial\Omega = \{ r(\theta, \phi) (\sin(\theta) \cos(\phi), \sin(\theta) \sin(\phi), \cos(\theta)) , \phi \in [0, 2\pi], \theta \in [0, \pi] \},$$

where  $r$  is expanded in terms of spherical harmonics

$$r(\theta, \phi) = \sum_{l=0}^N \sum_{m=-l}^l a_{l,m} y_l^m(\theta, \phi),$$

where

$$y_l^m(\theta, \phi) = \begin{cases} \sqrt{2} k_l^m \cos(m\phi) P_l^m(\cos(\theta)) & \text{if } m > 0, \\ k_l^0 P_l^0(\cos(\theta)) & \text{if } m = 0, \\ \sqrt{2} k_l^m \sin(-m\phi) P_l^{-m}(\cos(\theta)) & \text{if } m < 0, \end{cases}$$

$P_l^m$  is an associated Legendre polynomial and

$$k_l^m = \sqrt{\frac{(2l+1)(l-|m|)!}{4\pi(l+|m|)!}}.$$

Then, we collect all the coefficients  $a_{l,m}$  in a single vector

$$\mathcal{C} = (a_{0,0}, a_{1,-1}, a_{1,0}, a_{1,1}, a_{2,-2}, a_{2,-1}, a_{2,0}, a_{2,1}, a_{2,2}, \dots).$$

The shape optimization is solved by searching for optimal vectors  $\mathcal{C}$  using a gradient type method. In this context, a key ingredient is the Hadamard formula of derivation with respect to the domain (e.g. [361]). Consider an application  $\Psi(t)$  such that

$$\Psi : t \in [0, T) \rightarrow W^{1,\infty}(\mathbb{R}^N, \mathbb{R}^N) \text{ is differentiable at } 0 \text{ with } \Psi(0) = I, \Psi'(0) = V,$$

where  $W^{1,\infty}(\mathbb{R}^N, \mathbb{R}^N)$  is the set of bounded Lipschitz maps from  $\mathbb{R}^N$  into itself,  $I$  is the identity and  $V$  is a deformation field. We denote by  $\Omega_t = \Psi(t)(\Omega)$ ,  $\lambda_k(t) = \lambda_k(\Omega_t)$ , and by  $u$  an associated normalized eigenfunction. If we assume that  $\Omega$  is of class  $C^2$  and  $\lambda_k(\Omega)$  is simple, then

$$\lambda_k'(0) = - \int_{\partial\Omega} \left( \frac{\partial u}{\partial n} \right)^2 V \cdot n d\sigma. \quad (21)$$



For the Neumann case, assuming that  $\Omega$  is of class  $C^3$ ,  $\mu_k$  is simple and  $u$  is the associated normalized eigenfunction, we have

$$\mu'_k(\Omega)(0) = \int_{\partial\Omega} (|\nabla u|^2 - \mu_k u^2) V.nd\sigma. \quad (22)$$

### 3 The menagerie of the spectrum

In this section we present the main numerical results that we gathered for the solution of the shape optimization problems (1) and (2). In Figure 1 we plot the minimizers of the first 15 Dirichlet eigenvalues.

Table ?? shows the optimal Dirichlet eigenvalues, together with the corresponding multiplicity of each optimal eigenvalue.

**Table 1.** The optimal Dirichlet eigenvalues  $\lambda_i^*$ , for  $i = 1, 2, \dots, 15$  and the multiplicity of the optimal eigenvalue.

$i$	multiplicity	$\lambda_i^*$
1	1	18.17
2	2	36.34
3	3	46.13
4	3	64.30
5	2	78.15
6	3	88.48
7	3	106.12
8	3	118.88
9	3	132.34
10	4	142.69
11	4	159.40
12	4	172.88
13	4	186.91
14	4	198.94
15	5	209.62

In Figure 2 we plot the maximizers of the first 10 (non trivial) Neumann eigenvalues in the class of unions of simply connected domains.

Table ?? shows the optimal Neumann eigenvalues and the corresponding optimal multiplicity.

Next, we present some numerical results for the shape optimization problems (1) and (2) with three-dimensional domains. In Figure 3 we plot the 3D minimizers of the first 10 Dirichlet eigenvalues. Table ?? shows the optimal 3D Dirichlet eigenvalues and

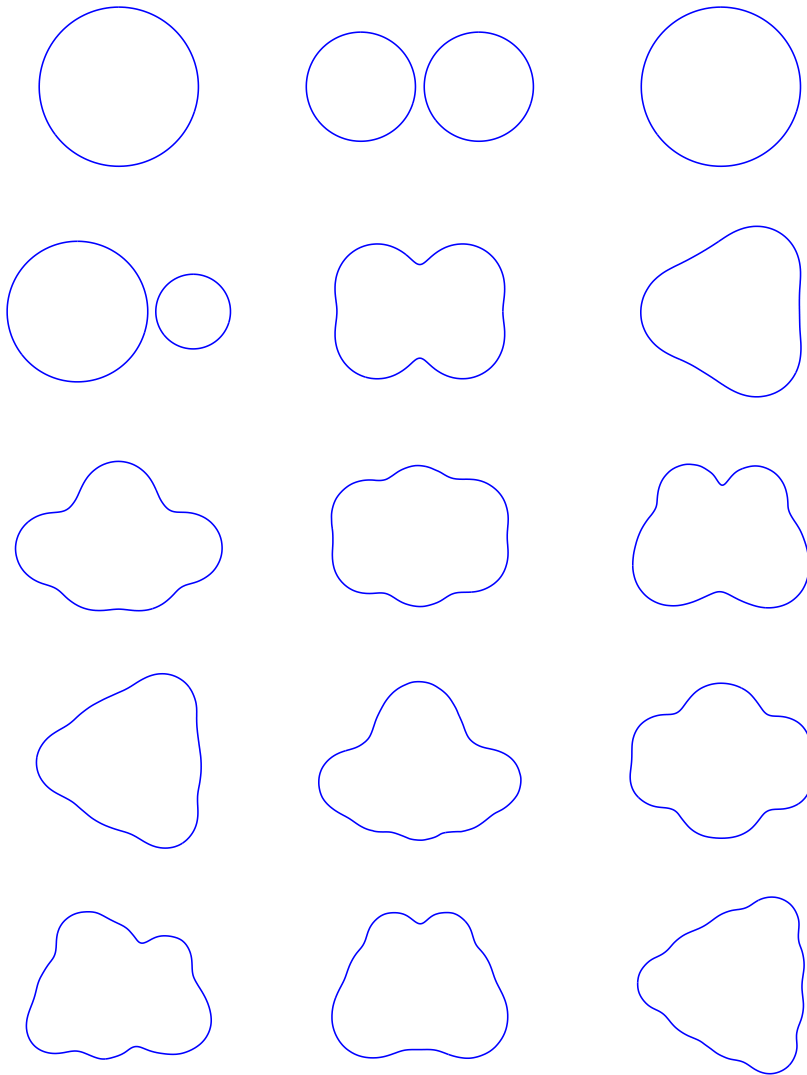


**Fig. 1.** The minimizers of the first 15 Dirichlet eigenvalues.

the corresponding multiplicity. Figure 4 and Table ?? show similar results for Neumann eigenvalues.

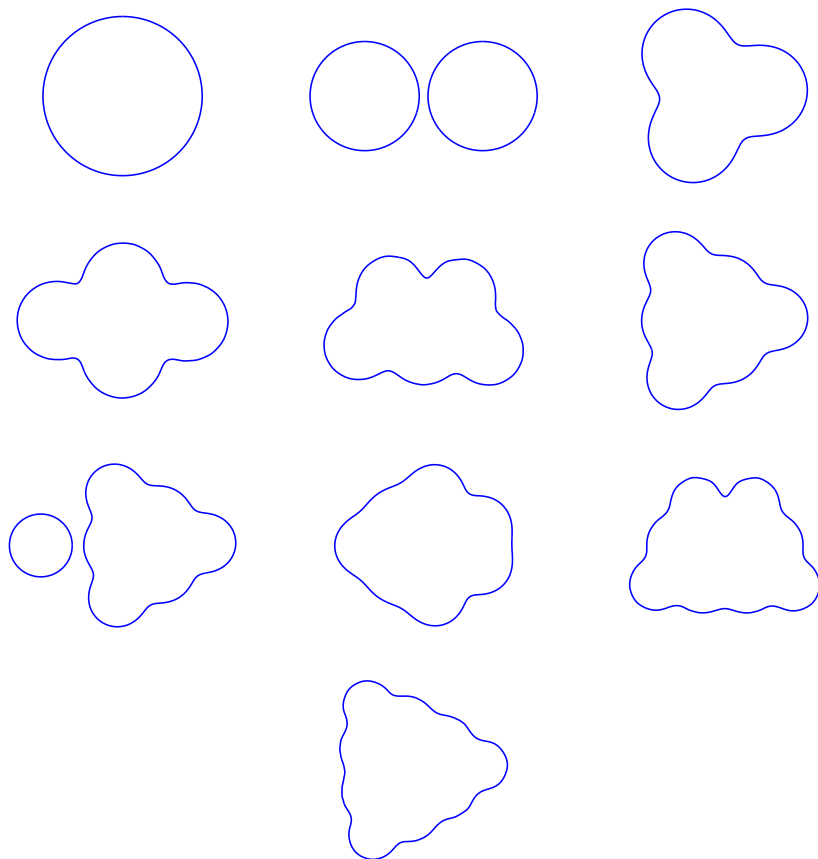


Fig. 2. The maximizers of the first 10 (non trivial) Neumann eigenvalues.

## 4 Open problems

The numerical results that we obtained suggest some conjectures

**Open problem 4.1.** *Prove that the  $d$ -dimensional ball minimizes  $\lambda_{d+1}$  among all  $d$ -dimensional sets of a fixed volume.*

**Open problem 4.2.** *Prove that the  $d$ -dimensional minimizer of  $\lambda_{d+2}$  among all  $d$ -dimensional sets of a fixed volume is the union of two balls whose radii are in the ratio*

$$\frac{j_{\frac{d}{2},1}}{j_{\frac{d}{2}-1,1}},$$

where  $j_{n,k}$  is the  $k$ -th zero of the Bessel function  $J_n$ .

**Table 2.** *The optimal Neumann eigenvalues  $\mu_i^*$ , for  $i = 1, 2, \dots, 11$  and the corresponding multiplicity.*

$i$	multiplicity	$\mu_i^*$
2	2	10.66
3	4	21.28
4	3	32.90
5	3	43.86
6	3	55.17
7	4	67.33
8	6	77.99
9	4	89.38
10	4	101.83
11	5	114.16

**Table 3.** *The optimal 3D Dirichlet eigenvalues  $\lambda_i^*$ , for  $i = 1, 2, \dots, 10$  and the corresponding multiplicity.*

$i$	multiplicity	$\lambda_i^*$
1	1	25.65
2	2	40.72
3	2	49.17
4	3	52.47
5	4	63.83
6	3	73.05
7	4	78.35
8	6	83.29
9	5	86.32
10	3	92.33

**Acknowledgment:** The research of the first author was partially supported by FCT, Portugal, through the program “Investigador FCT” with reference IF/00177/2013 and the scientific project PTDC/MAT-CAL/4334/2014.

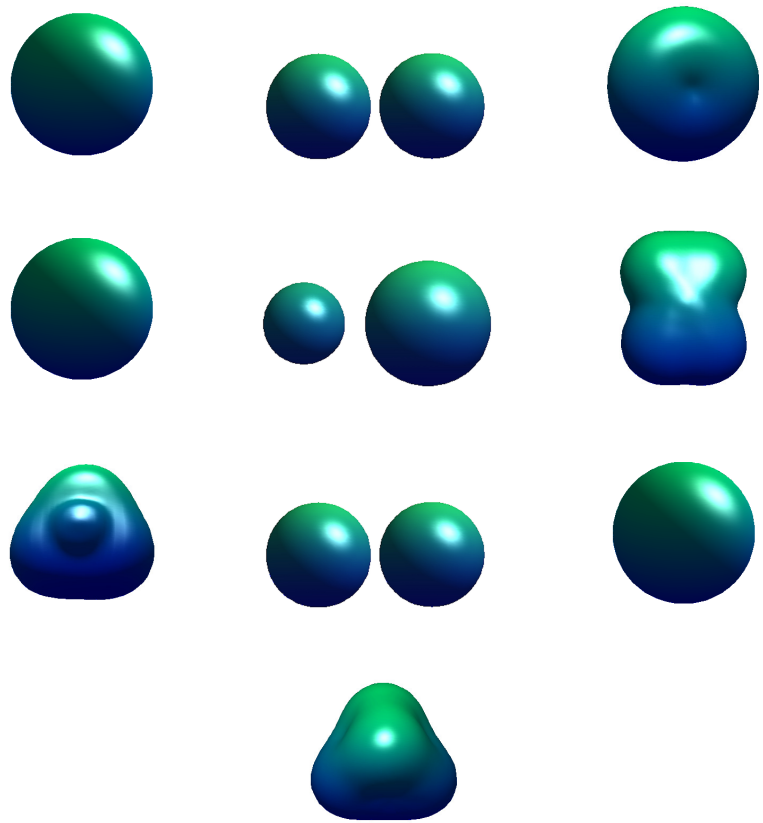


**Fig. 3.** The 3D minimizers of the first 10 Dirichlet eigenvalues.

**Table 4.** The optimal 3D Neumann eigenvalues and the corresponding multiplicity.

$i$	multiplicity	$\mu_i^*$
2	3	11.25
3	6	18.87
4	4	23.52
5	5	29.02
6	5	33.55
7	4	37.83
8	3	41.18
9	3	46.63
10	4	52.49
11	7	55.91

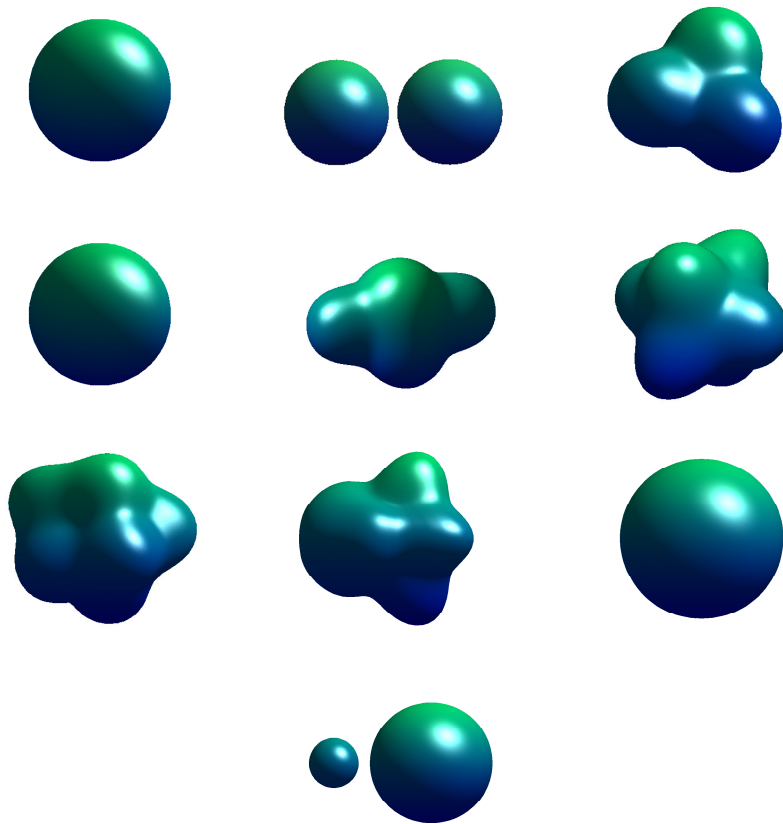


**Fig. 4.** The 3D maximizers of the first 10 (non trivial) Neumann eigenvalues.

